ACS OMEGA

http://pubs.acs.org/journal/acsodf

Article

Artificial Intelligence Techniques and Response Surface Methodology for the Optimization of Methyl Ester Sulfonate Synthesis from Used Cooking Oil by Sulfonation

Adeyinka Sikiru Yusuff,* Niyi Babatunde Ishola,* and Afeez Olayinka Gbadamosi

Cite This: *ACS Omega* 2023, 8, 19287−19301

Read Online

ACCESS | Metrics & More | Article Recommendations

ABSTRACT: Herein, the impacts of sulfonation temperature (100−120 °C), sulfonation time (3−5 h), and $NaHSO_3$/methyl ester (ME) molar ratio (1:1−1.5:1 mol/mol) on methyl ester sulfonate (MES) yield were studied. For the first time, MES synthesis via the sulfonation process was modeled using the adaptive neuro-fuzzy inference system (ANFIS), artificial neural network (ANN), and response surface methodology (RSM). Moreover, particle swarm optimization (PSO) and RSM methods were used to improve the independent process variables that affect the sulfonation process. The RSM model (coefficient of determination (R^2) = 0.9695, mean square error (MSE) = 2.7094, and average absolute deviation (AAD) = 2.9508%) was the least efficient in accurately predicting MES yield, whereas the ANFIS model (R^2 = 0.9886, MSE = 1.0138, and AAD = 0.9058%) was superior to the ANN model (R^2 = 0.9750, MSE = 2.6282, and AAD = 1.7184%). The results of process optimization using the developed models revealed that PSO outperformed RSM. The ANFIS model coupled with PSO (ANFIS-PSO) achieved the best combination of sulfonation process factors (96.84 °C temperature, 2.68 h time, and 0.92:1 mol/mol $NaHSO_3$/ME molar ratio) that resulted in the maximum MES yield of 74.82%. Analysis of MES synthesized under optimum conditions using FTIR, ^{1}H NMR, and surface tension determination showed that MES could be prepared from used cooking oil.

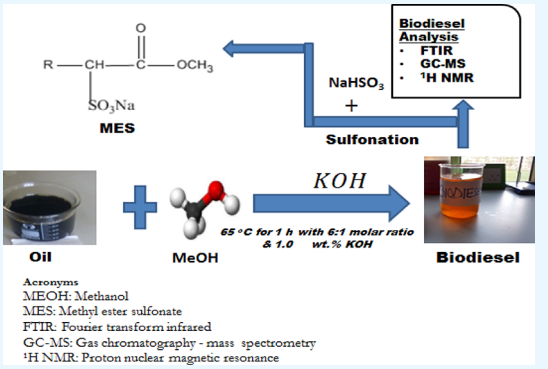

1. INTRODUCTION

The search for biodegradable and renewable feedstock for commercial production has been a research focus in recent time due to the depleting nature of crude oil and the necessity to safeguard the environment from the toxicity of petrochemical products.[1,2] Vegetable oil, algal oil, animal fat, and used cooking oil (UCO) are renewable and biodegradable feedstocks that can replace finite petroleum-based chemicals. UCO is a low-quality raw material whose use could reduce the cost of producing biodiesel (an intermediate product of methyl ester sulfonate). Besides, the processing of UCO aids in the effective conversion of biomass to useful products.[3,4] Currently, large volumes of UCO are produced around the world and pose a waste disposal issue.[5,6] As a result, there is a need to develop an innovative technology for collecting UCO from various locations and using it as a feedstock in the commercial production of fatty acid methyl ester (FAME) for surfactant (methyl ester sulfonate, MES) synthesis.[1,7]

Surfactants are derived from either petrochemicals or oleochemicals.[1] Surfactants derived from bio-oils have been found to be nontoxic, less viscous, biodegradable, soluble in water, and slightly irritant to humans[4,8] when compared to petroleum-based surfactants such as cetyltrimethylammonium-bromide (CTAB), internal olefin sulfonate (IOS), and sodium dodecyl sulfate (SDS), which may soon be phased out owing to the depletion of crude oil reserves.[7,9] One of the kinds of oleochemical-based surfactants is fatty acid methyl ester sulfonate (MES).

MES is an anionic surfactant made by either direct sulfonation of FAME with a sulfonating agent such as SO_3, chlorosulfonic acid, oleum, or $NaHSO_3$ or neutralization of fatty acid methyl ester sulfonic acid (MESA) with sodium hydroxide.[4,9] Although the air-SO_3 falling film sulfonation process is efficient for MES production, it can only be done on a large scale continuously. However, because the former can be run batch-wise or continuously, the $NaHSO_3$-based sulfonation process has been proposed as a viable alternative to the air-SO_3 falling film sulfonation method. Furthermore, unlike air-SO_3 falling film sulfonation, the $NaHSO_3$-methyl ester sulfonation

Received: December 22, 2022
Accepted: March 24, 2023
Published: May 24, 2023

process does not release heat.[10,11] Wibowo et al.[12] reported MES synthesis via sulfonation of palm oil methyl esters with $NaHSO_3$, with an MES yield of 93.2%. Using the $NaHSO_3$ sulfonation process, a novel castor oil fatty acid methyl ester ethoxylate sulfonate was synthesized.[13] When UCO methyl ester was sulfonated with $NaHSO_3$, a sulfonated product with improved properties was formed.[7]

Numerous studies have explored the use of conventional methods to assess the factors influencing the sulfonation process. Using this approach, experimental runs were performed by methodically changing the examined variable while maintaining the other variables constant. The performance ability of response surface methodology (RSM) in the sulfonation process has previously been reported.[7] The use of conventional methods is characterized by several uncertainties. For example, although RSM can be used to lower experimental runs required to examine the impacts of various input factors and their combined influence on the response, it is unable to capture a chemical or biological process' nonlinear behavior. Moreover, all of the contributing factors must be tested again, which result in a doubtful number of experimental runs.

More recently, robust statistical modeling tools of artificial intelligence techniques such as the adaptive neuro-fuzzy inference system (ANFIS) and artificial neural network (ANN) have been exploited for modeling processes because they can be used to approximate the nonlinearity associated to a biochemical process system. ANN imitates the brain process mechanism and hence consists of a group of neurons that are linked together in multiple layers. These multiple layers form the basis of the ANN and are referred to as multilayered perceptron (MLP) comprising three layers, *viz.*, input, hidden, and output layers. A benefit of ANN is that it may estimate a variety of nonlinear functions without the need for a specific fitting function to be specified.[14] ANN has been employed in various chemical processes, such as enzymatic-catalyzed reactions,[15,16] esterification and transesterification reaction for biodiesel synthesis,[17−20] polymerization reactions,[21,22] and the photocatalytic process.[23] ANFIS is a technique that combines both fuzzy systems and neural networks in a single framework. This offers the ANFIS an advantage such as the ability to demonstrate ambiguity, learning steps, as well as the computational power of neural networks.[24] It has also been used in various chemical processes.[25−28] Advantages of ANN and ANFIS compared to RSM have been extensively reported in many studies.[18,19,23,29,30]

To increase the effectiveness of the process, it is essential to optimize the process parameters.[31] Due to the local optimization method by RSM that is only capable of searching local optima, a global optimization method such as particle swarm optimization (PSO) is needed that would locate the global optimum of a given function. PSO is a renowned metaheuristic population-based approach. It is a stochastic optimization technique that is based on the swarm behavior such as flocking of birds and schooling fish. Whereas RSM has its own inbuilt optimization algorithm, ANN and ANFIS developed models need to be coupled with PSO to estimate the global optima of a process. It is noteworthy to state that there has not been a report in the open literature in the optimization of the sulfonation process using the trio of RSM-PSO, ANN-PSO, and ANFIS-PSO.

Thus, methyl ester sulfonate synthesis via sulfonation of methyl ester (ME) with $NaHSO_3$ was modeled using the trio of ANFIS, ANN, and RSM optimization techniques. The influence of temperature, time, and molar ratio of $NaHSO_3$ to ME on the sulfonation process was investigated. The effectiveness of the methods was determined statistically by employing the average absolute deviation (AAD), correlation coefficient (R), coefficient of determination (R^2), adjusted R^2, and mean square error (MSE). Furthermore, ME and MES produced under optimum conditions were characterized using FTIR, ^{1}H NMR, GC-FID, and surface tension determination analyses.

2. METHODOLOGY

2.1. Materials. UCO utilized for the experiment was obtained from an eatery in Dehradun, India. The procedure used in pretreating the oil sample and its physicochemical properties have been previously reported.[7] All the chemical

Table 1. Experimental Ranges and Levels of the Operational Parameters

		level				
parameter	description	$-\alpha$	−1	0	+1	$+\alpha$
T	sulfonation temperature (°C)	96.84	100	110	120	123.16
t	sulfonation time (h)	2.68	3.0	4.0	5.0	5.32
M	$NaHSO_3$/ME molar ratio (mol/mol)	0.92:1	1:1	1.25:1	1.5:1	1.58:1

Table 2. Features of the Developed ANN and ANFIS Model

model	property	value/remark
ANN	training function	Levenberg−Marquardt backpropagation
	performance function	MSE
	learning	supervised
	input layer transfer function	no transfer function is used
	output layer transfer function	purelin
	hidden layer transfer function	hyperbolic tangent sigmoid (tansig)
	number of training iterations	120
	number of best iterations	70
	number of input neurons	3[a]
	number of hidden neurons	10
	number of output neurons	1[b]
ANFIS	fuzzy type	Sugeno
	input	3[a]
	output	1[b]
	membership function	generalized bell-shaped
	input/ouput membership function	3
	and method	product
	or method	probabilistic
	implication method	product
	aggregation	sum
	number of rules	27
	number of of linear parameters	54
	number of nonlinear parameters	27
	output membership function type	linear

[a]Sulfonation temperature, sulfonation time, and $NaHSO_3$/ME molar ratio. [b]MES yield.

https://doi.org/10.1021/acsomega.2c08117
ACS Omega 2023, 8, 19287−19301

Table 3. Weights of ANN Model Employed for Analysis Results

	input weights			output weight
neuron	sulfonation temperature	sulfonation time	$NaHSO_3$/ME	MES yield
1	2.3174	1.6698	−1.0946	0.6126
2	2.2292	1.9752	−1.3210	1.1358
3	−2.3596	1.1338	−0.7228	0.3221
4	−2.3942	−1.1341	1.2867	−0.0173
5	−3.6142	1.1097	0.1621	1.8098
6	−1.4673	2.9082	0.9966	−1.1542
7	1.2220	−1.7860	1.7769	0.3842
8	2.5357	−0.8107	1.8620	0.9540
9	1.1485	1.7165	−1.9031	−0.2252
10	−1.4492	−1.3038	1.6817	−0.0526

Table 4. ANFIS Sensitivity Analysis Parameters

input variable	minimum	nominal	maximum
temperature	96.84	110	123.16
time	2.68	4	5.32
$NaHSO_3$/ME molar ratio	0.92	1.25	1.58

Table 5. PSO Features for RSM, ANN, and ANFIS Developed Models

property	value/comment
swarm size	10−15
initial range	[0.1, 0.1]
self-adjustment	2
social adjustment	2
iteration	10−50

compounds (KOH, CH_3OH, $NaHSO_3$, Al_2O_3, and NaOH) herein were provided by Thermo-Fisher Scientific Industries, Mumbai, India.

2.2. Preparation of ME and MES. *2.2.1. ME Synthesis.* The methanolysis process was used to convert UCO to methyl esters in a round-bottom flask. The process was carried out at a temperature of 65 °C for a duration of 1 h. The molar ratio of UCO to methanol was 1:6, and KOH was used as catalyst with a concentration of 1.0 wt %. After completing the reaction process, the resulting product was separated into two layers (upper and lower layers) via a separating funnel. Subsequently, the upper layer (a mixture of biodiesel and unreacted methanol) was evaporated in a rotary vacuum evaporator to remove methanol. Thereafter, the produced biodiesel was washed severally with warm water to remove dissolved KOH and finally dried to remove moisture.

2.2.2. MES Synthesis. MES was synthesized using the method described by Wibowo et al.,[12] that is, sulfonation of UCO methyl esters with $NaHSO_3$ in a two-neck round bottom flask with a magnetic stirrer. ME, $NaHSO_3$, and alumina (as catalyst) were fed to the reaction vessel and stirred at 400 rpm. The operating parameters (molar ratio of $NaHSO_3$ to ME, time, and temperature) were adjusted to the desired operating values (see Table 1). When the sulfonation reaction was completed, a centrifuge was employed to remove the residual $NaHSO_3$ at a rotating speed of 7500 rpm for 20 min. Afterward, the methyl ester sulfonic acid (MESA) obtained from the supernatant was purified with methanol for 1.5 h at 55 °C. Finally, the purified product was neutralized by adding the 20% NaOH solution dropwise while stirring until a pH of about 8.0 was achieved. After methanol recovery with a rotary evaporator, a sticky pale yellow liquid product (MES) was kept in a covered container for quality analysis. The MES yield (Y_1) was calculated as the percentage of the mass of MES obtained (M_{MES}) to the mass of ME used (M_{ME}).

$$Y_1 = \frac{M_{MES}}{M_{ME}} \times 100\,\% \tag{1}$$

2.3. Model Development. *2.3.1. Sulfonation Process Optimization by RSM.* The central composite design (CCD) of RSM was utilized to generate the data set for conducting the experiment. To examine the influence of operational parameters on the sulfonation process output (MES yield), three numeric parameters (sulfonation temperature, sulfonation time, and $NaHSO_3$/ME molar ratio) were selected. Fifteen experimental runs were suggested by the CCD as indicated in Table 1, which were replicated twice, and the average result of the decolorization efficiency was reported.

The response and operational parameters were correlated using a second-order polynomial response equation (eq 2) with all model terms.

$$Y = \beta_o + \beta_1 A + \beta_2 B + \beta_3 C + \beta_{12} AB + \beta_{13} AC + \beta_{23} BC + \beta_{11} A^2 + \beta_{22} B^2 + \beta_{33} C^2 \tag{2}$$

where Y stands for the process output (MES yield), β_o symbolizes the constant coefficient; β_1, β_2, and β_3 are the linear terms; β_{12}, β_{13}, and β_{23} are the coefficients of interaction terms; β_{11}, β_{22}, and β_{33} denote the coefficients of quadratic terms; and T, t, and M are the coded values of the sulfonation process variables.

2.3.2. Development of the Sulfonation Process' ANN Model. Levenberg−Marquardt's algorithm (LMA) was used to create a feedforward, multilayer ANN because of its ability for quick convergence and function modeling. Pure-linear (purelin) and hyperbolic tangent sigmoid (tansig) transfer functions were used for the input−output−hidden layers, respectively. The chosen ANN had an input layer consisting of three neurons (sulfonation temperature, sulfonation time, and $NaHSO_3$/methyl ester (ME) molar ratio) and a hidden−output layer with one neuron (MES yield). Iteratively testing different numbers of neurons (2−20) until the mean square error (MSE) value of the target data was minimal and high R, which is nearly equal to unity, was attained was used to obtain the optimal hidden neuron number. The tangent sigmoid function is described by eq 3, whereas the purelin transfer is given by eq 4.

$$\text{tansig}(w) = \frac{2}{(1 + e^{-2w})} - 1 \tag{3}$$

$$f(w) = w \tag{4}$$

Every input and output data set was scaled back to a value between −1 and +1. Because the tangent sigmoid transfer function varies from −1 to +1, normalization is required. In addition, the normalization ensures that overflow that may result to very large or very small weight anomalies is avoided.[32] The normalization was performed by using eq 5.

$$\text{Normalized} = \frac{2(X^A - X^{min})}{(X^{max} - X^{min})} \tag{5}$$

https://doi.org/10.1021/acsomega.2c08117
ACS Omega 2023, 8, 19287−19301

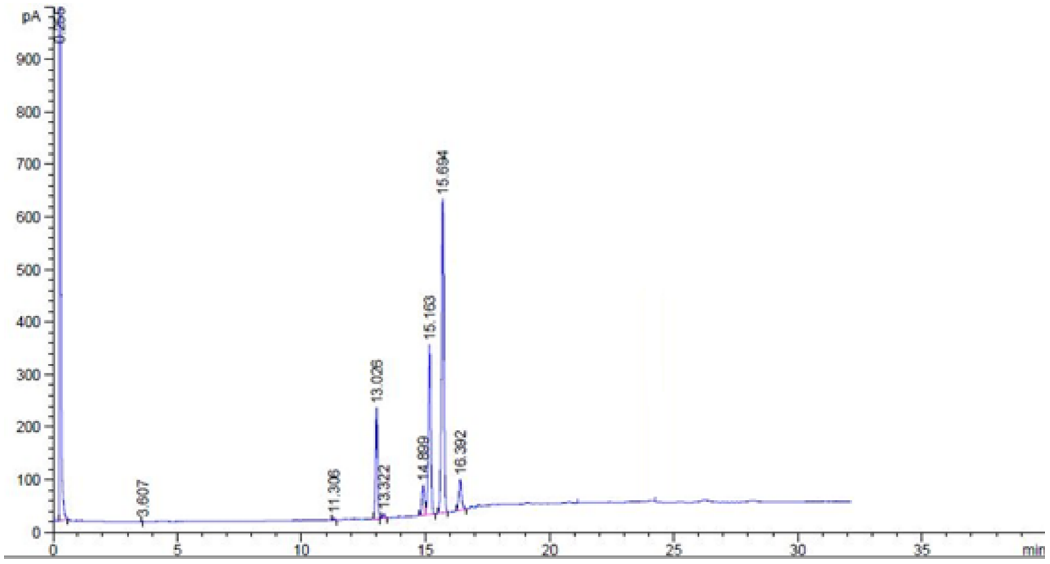

Figure 1. Chromatogram of UCO methyl ester.

where X^{A}, X^{min}, and X^{max} signify the actual, minimum, and maximum, respectively.

The data set points of input and output (15 in total) were grouped into three subsets, *viz.*, training (60%), validation (20%), and testing (20%).[33] This is crucial to determine the model's capacity for predicting hidden data that were not used for training and to evaluate the ANN's capacity for generalization.[34]

2.3.3. Development of the Sulfonation Process' ANFIS Model. To prognosticate the MES yield of the sulfonation process, the multiple-input−single-output (MISO) fuzzy model was used to implement the ANFIS model. Three inputs (sulfonation temperature, sulfonation time, and $NaHSO_3$/ME molar ratio) and one output (MES yield) were employed to develop the ANFIS model. Three generalized bell-shaped membership functions (*gbellmf*) of first-order Sugeno fuzzy logic were employed for each of the input factor. The output prediction of the ANFIS model was done using hybrid learning algorithms integrated with the defuzzifier formular. The framework was built employing normalization, defuzzification and fuzzification, overall summation, and product.[35] The Takagi−Sugeno IF−THEN rules with regard to the input variables can be defined using rules 1 and 2, assuming a two input variable fuzzy inference system (FIS) (u and v) and an output (w).[35] The following expression is given for rules 1 and 2:

Rule 1: IF u is A_1 and v is B_1,

$$\text{THEN } e_1 = g_1 u + h_1 v + k_1$$

Rule 2: IF u is A_2 and v is B_2,

$$\text{THEN } e_2 = g_2 u + h_2 v + k_2$$

where the fuzzy sets are A_1, A_2, B_1, and B_2 and the outputs of the system are u_1 are u_2. The controllable parameters of the FIS are g_1, g_2, h_1, h_2, k_1, and k_2.

2.3.3.1. First Layer. This layer contains adaptive nodes with three input parameters. Each node n is defined by the following function:

$$\psi_n^1 = \alpha_{A_n}(u) \tag{6}$$

where the input parameter to node n is designated as u and ψ_n^1 (symbolizes MF) is the fuzzy set. A_n is the membership class that implies when the provided input n satisfies A.

The expression of *gbellmf* is given as

$$\alpha_{A_n}(u) = \frac{1}{1 + \left|\frac{u - k_n}{g_p}\right|^{2h_n}} \tag{7}$$

where *gbellmf* premise parameters are g_p, h_p, and k_p. The width of the curve is modified by g and h (both must ≥ 0), and k is the curve's midpoint. The MF values vary between 0 and 1.

2.3.3.2. Second Layer. This region contains nonadaptive nodes. Product of the incoming signals is performed in this layer to subject all the weight (μ) to scrutiny. Each output node demonstrates the firing strength of the weight.

$$\psi_n^2 = \mu_n = \alpha_{A_n}(u)_n \cdot \alpha_{B_n}(u)_n, n = 1, 2 \tag{8}$$

2.3.3.3. Third Layer. Each node runs the required fuzzy rules, and this layer computes each level activation rule. This layer is evaluated by dividing the firing strength of each rule by the aggregate number of rules. This layer's node is not adaptable.

$$\psi_n^3 = \overline{\mu}_n = \frac{\mu_n}{\mu_1 + \mu_2}, n = 1, 2 \tag{9}$$

2.3.3.4. Fourth Layer. Defuzzification is used in this layer to calculate the output of the membership function. This layer's nodes are adaptable.

$$\psi_n^4 = \overline{\mu}_n \cdot Q_n = \overline{\mu}_n (g_n u + h_n v + k_n), n = 1, 2 \tag{10}$$

where $[g_p, h_p, k_p]$ refers to a consequent parameter set.

2.3.3.5. Fifth Layer. This has the total of the individual node's outputs from the defuzzification layer. A single node that represents the output indicates that the layer is not adaptable.

$$\psi_n^5 = \sum_n \overline{\mu}_n \cdot Q_n = \frac{\sum_n \mu_n \cdot Q_n}{\sum_n \mu_n}, n = 1, 2 \tag{11}$$

https://doi.org/10.1021/acsomega.2c08117
ACS Omega 2023, 8, 19287−19301

Table 6. Composition of the FAME Intermediate Derived from UCO

FAME profile	chemical formula	retention time (min)	composition (wt %)	class
methyl myristate	$C_{15}H_{30}O_2$	11.308	0.7	unsaturated
methyl palmitate	$C_{17}H_{34}O_2$	12.672	13.7	saturated
methyl palmtoleate	$C_{17}H_{32}O_2$	13.589	0.20	unsaturated
methyl stearate	$C_{19}H_{38}O_2$	14.662	5.4	saturated
methyl oleate	$C_{19}H_{36}O_2$	14.839	23.7	unsaturated
methyl linoleate	$C_{19}H_{34}O_2$	15.319	47.2	unsaturated
methyl linolenate	$C_{19}H_{32}O_2$	16.000	5.8	unsaturated
total saturated (%)			19.1	
total unsaturated (%)			77.6	
total FAME (%)			96.7	
other			3.3	

where $\bar{\mu}_n$. Q_n denotes the output of node n in the defuzzification layer. Table 2 summarizes the ANFIS features that were employed in this study. The modeling of the ANFIS was carried out in MATLAB 2018a using the fuzzy logic toolbox.

2.4. Operational Parameters' Sensitivity Study. Conducting a sensitivity study will ensure how well the model behaves. It is used to examine the impact of each input parameter on the model response (output).[36] The sum of squares for each input term and the total of squares for all input parameters were used to conduct the sensitivity analysis for the RSM model.[37] These sums of squares were utilized to compute the percentage contribution of each input parameter on the response (MES yield) following eq 12.

$$\%\ \text{Input parameter contribution} = \frac{\text{SOS}_i}{\text{SOS}_o} \tag{12}$$

where SOS_i and SOS_o, respectively, represent the sum of squares for a particular input factor and the total sum of squares for all the input factors.

Sensitivity analysis of the input factors for the implemented ANN model was carried out employing Garson's method following eq 13.[38] The weights computed for both the input parameters and the response (MES yield) are displayed in Table 3. The calculated weights were employed to analyze the relative importance of the operational factors.

$$\Omega_t = \frac{\sum_{a=1}^{a=n_h}\left(\left(\frac{|\beta_{ta}^{ih}|}{\sum_{k=1}^{n_i}|\beta_{ka}^{ih}|}\right)\times|\beta_{ab}^{ho}|\right)}{\sum_{k=1}^{k=n_i}\left\{\sum_{a=1}^{a=n_h}\left(\frac{|\beta_{ka}^{ih}|}{\sum_{k=1}^{n_i}|\beta_{ka}^{ih}|}\right)\times|\beta_{ab}^{ho}|\right\}} \tag{13}$$

where the terms n_i and n_h symbolize the input and hidden neurons, respectively. The connecting weight is represented by β. The layers consisting of the input, hidden are designated by i, h, and o superscripts, respectively, whereas neurons embedded in the input, hidden, and output are symbolized by the k, a, and b subscripts. Ω_t is the t_{th} input parameter's influence on the output parameter's relative importance.

The ANFIS model's input parameters were analyzed for sensitivity by determining the maximal value of the selected input parameters while retaining the remaining input parameters at their nominal levels (the most frequent values). The sensitivity study was carried out to validate the effect of input parameters on the model response (MES yield) of the implemented ANFIS model. To depict the response of the ANFIS model, one variable was changed, whereas other variables remained constant.[39] Table 4 displays the nominal, minimum, and maximal values that were employed to perform the sensitivity analysis by the ANFIS model.

2.5. Process Parameter Optimization. The optimization procedures of RSM and PSO were engaged to determine the optimal blends of process variables to attain the highest MES yield to improve the sulfonation process. The implemented ANN, ANFIS, and RSM models were used as the optimization algorithm's fitness function. Table 5 illustrates parameters of PSO employed for the variables' optimization. The optimal values prognosticated by RSM and PSO were validated in the lab by completing the experiment in triplicate separately. By averaging the values, the observed values and predicted values

Table 7. The Three-Factor CCD Matrix and the Value of Prediction by the Developed Models

run	sulfonation temperature, T (°C)	sulfonation time, t (h)	$NaHSO_3$/ME molar ratio, M (mol/mol)	MES yield (wt %)	RSM prediction (wt %)	ANN prediction (wt %)	ANFIS prediction (wt %)
1	123.16	4	1.25	58.1	59.68	62.71	58.10
2	96.84	4	1.25	38.5	40.08	38.50	38.50
3	100	3	1	70	68.63	69.98	70.00
4	120	3	1.5	38.51	37.14	38.51	38.51
5	110	2.68	1.25	49.8	51.37	49.80	49.80
6	100	5	1.5	57.2	55.83	57.21	57.20
7	110	4	1.58	41.5	43.07	41.50	41.50
8	110	5.32	1.25	65	66.57	65.02	65.00
9	110	4	0.92	42.8	44.37	41.78	42.80
10	120	5	1	60	58.63	61.38	60.00
11	110	4	1.25	45.7	45.05	45.72	45.84
12	110	4	1.25	45	45.05	45.72	45.84
13	110	4	1.25	45.8	45.05	45.72	45.84
14	110	4	1.25	49	45.05	45.72	45.84
15	110	4	1.25	43.72	45.05	45.72	45.84

https://doi.org/10.1021/acsomega.2c08117
ACS Omega 2023, 8, 19287−19301

Table 8. Test of Significance for Every Regression Coefficient and ANOVA[a]

source	SS	df	MS	*F* value	*p* value	
model	1292.22	9	143.58	17.8686	0.0027	significant
T	192.08	1	192.08	23.9045	0.0045	
t	115.52	1	115.52	14.3766	0.0127	
M	0.845	1	0.845	0.10516	0.7588	
Tt	121.156	1	121.156	15.078	0.0116	
TM	24.0891	1	24.0891	2.99791	0.1439	
tM	396.736	1	396.736	49.3742	0.0009	
T^2	48.1694	1	48.1694	5.99473	0.0580	
t^2	403.473	1	403.473	50.2126	0.0009	
M^2	3.77958	1	3.77958	0.47037	0.5233	
ANOVA						
R^2	0.96985					
adjusted R^2	0.91557					
residual	40.1765	5	8.0353			
lack of fit	24.9698	1	24.9698	6.56809	0.0625	not significant
pure error	15.2067	4	3.80168			
total SS	1332.39	14				
adeq precision	13.6056					
CV (%)	5.66					

[a]SS, sum of squares; MS, mean square; df, degree of freedom; CV, coefficient of variation.

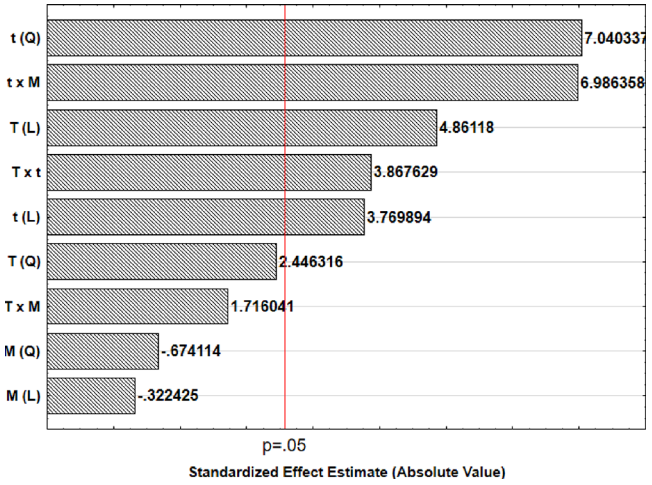

Figure 2. Pareto chart of standardized effects for the RSM model. *T*, sulfonation temperature; *t*, sulfonation time; *M*, $NaHSO_3$/ME molar ratio; *L*, linear; and *Q*, quadratic.

Table 9. Statistical Performance of the Developed Models

indicator	RSM	ANN	ANFIS
R	0.9846	0.9874	0.9943
R^2	0.9695	0.9750	0.9886
adj R^2	0.9584	0.9659	0.9844
MSE	2.7094	2.6282	1.0138
AAD (%)	2.9508	1.7184	0.9058

were compared. PSO codes were developed using MATLAB R2018a, while optimization by RSM was executed using version 7.0.0 of the Design Expert software.

2.6. Appraisal of the Developed ANN, ANFIS, and RSM Models. Statistical measures including the correlation coefficient (*R*), coefficient of determination (R^2), adjusted R^2, mean square error (MSE), and average absolute deviation (AAD) were engaged to evaluate the developed models' predictive efficacy. The statistical indicators were determined using eqs 14−18.[33,40]

$$R = \frac{\sum_{i=1}^{n}(x_{i,pr} - x_{ob,av})(x_{i,ob} - x_{i,pr})}{\sqrt{\sum_{i=1}^{n}[(x_{i,ob} - x_{i,pr})^2]\ \sum_{i=1}^{n}[(x_{i,pr} - x_{ob,av})^2]}} \quad (14)$$

$$R^2 = \frac{\sum_{i=1}^{n}(x_{i,ob} - x_{i,pr})^2}{\sum_{i=1}^{n}(x_{i,pr} - x_{ob,av})^2} \quad (15)$$

$$\text{Adjusted } R^2 = 1 - \left[(1 - R^2) \times \frac{n-1}{n-v-1}\right] \quad (16)$$

$$\text{MSE} = \frac{1}{n}\sum_{i=1}^{n}(x_{i,pr} - x_{i,ob})^2 \quad (17)$$

$$\text{AAD} = \frac{100}{n}\sum_{i=1}^{n}\frac{|(x_{i,ob} - x_{i,pr})|}{x_{i,ob}} \quad (18)$$

where *v* is the number of operational parameters, *n* is the experimental number points, $x_{i,\,pr}$ is the predicted value, $x_{i,\,ob}$ is the experimental value, and $x_{ob,\,av}$ is the mean of the observed value.

2.7. Analysis and Characterization of ME and MES. Transesterification and sulfonation processes' products were analyzed using different characterization techniques. A gas chromatography-flame ionization detector (Agilent 7890A, USA) and capillary column (size: 0.32 mm × 15 m, 0.10 mm thickness) were used in determining the FAME profile of the methanolysis product, as discussed in our previously reported study.[7] Furthermore, functional groups present in both methanolysis and sulfonation products were evaluated using Fourier transform infrared (FTIR) spectrophotometer (Perkin Elmer, USA), whereas the chemical compositions of the two products were analyzed with the aid of a nuclear magnetic resonance spectrometer (^{1}H NMR, Bruker Avance III-HD 500 MHz) with $CDCl_3$ used as solvent. A surface tensiometer (KRUSS Scientific, USA) was used to estimate the surface tension of the MES solution at different concentrations.

https://doi.org/10.1021/acsomega.2c08117
ACS Omega 2023, 8, 19287−19301

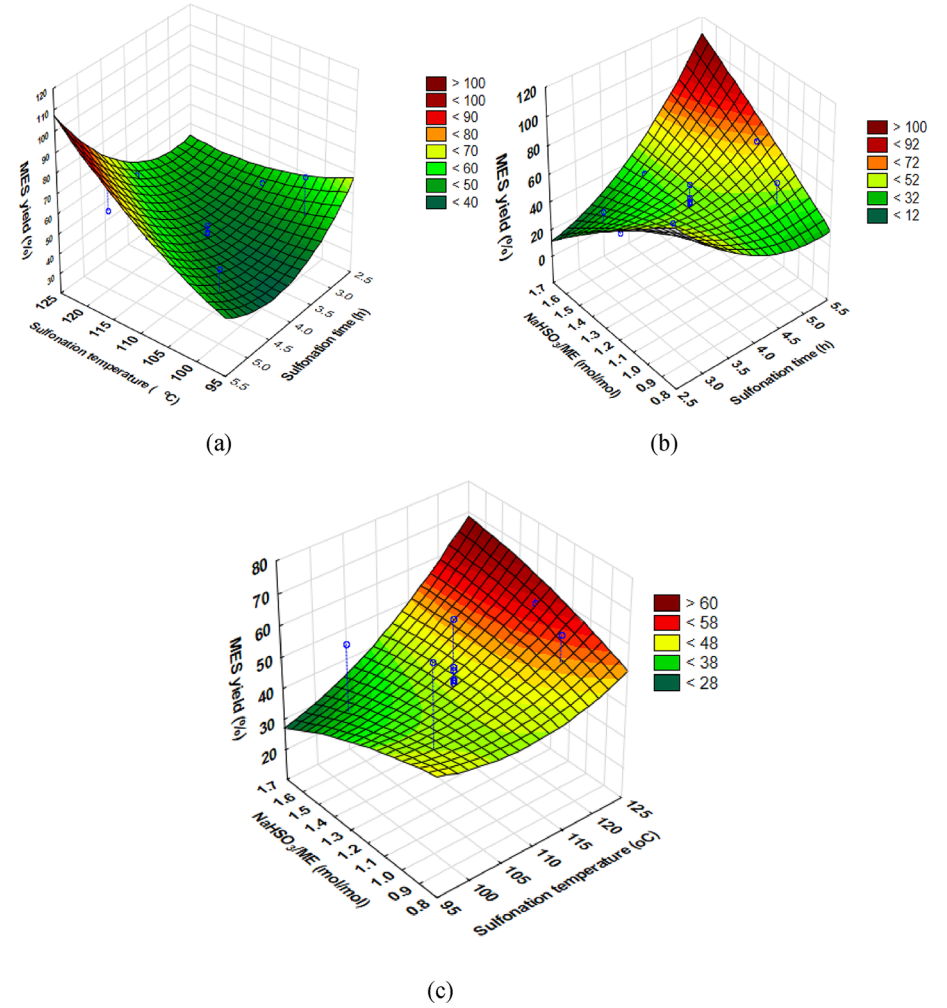

Figure 3. Surface plots on the impact of (a) sulfonation temperature (°C) and sulfonation time (h), (b) $NaHSO_3$/ME molar ratio and sulfonation time (h), and (c) $NaHSO_3$/ME molar ratio and sulfonation temperature (°C) on MES yield (%).

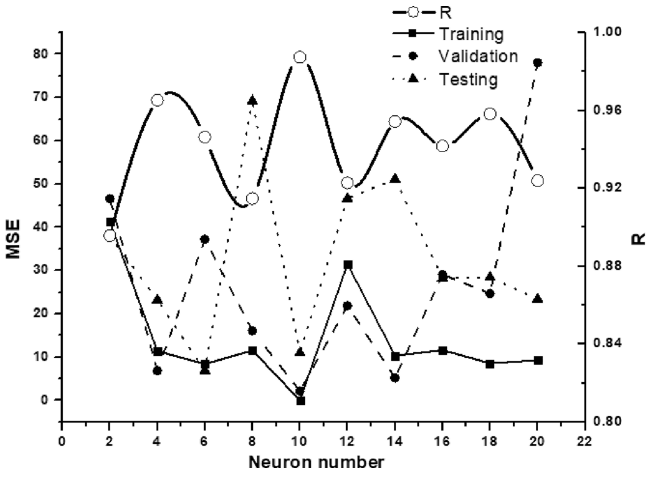

Figure 4. Optimal hidden neuron number.

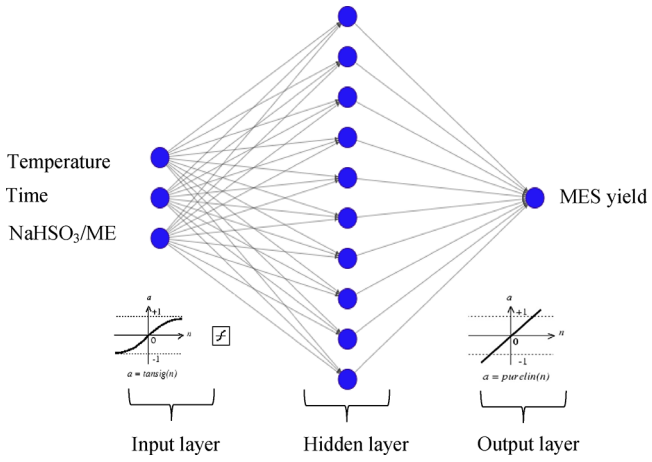

Figure 5. ANN topology with input, hidden (*tansig* transfer function), and output layers (pure linear transfer function).

3. RESULTS AND DISCUSSION

3.1. Analysis of FAME Profile of Biodiesel Produced from UCO. The GC-FID was used in analyzing the UCO methyl ester composition, and the analysis results are shown in Figure 1 and Table 6. As indicated in the results, the major methyl esters detected in the UCO biodiesel were palmitic, oleic, linoleic, linolenic, and stearic acids. The methyl linoleate accounted for 47.2% of the whole intermediate product, making it a dominant component in the synthesized UCO FAME. Furthermore, the GC-FID results revealed that the UCO biodiesel contained 19.10% saturated and 77.6%

https://doi.org/10.1021/acsomega.2c08117
ACS Omega 2023, 8, 19287−19301

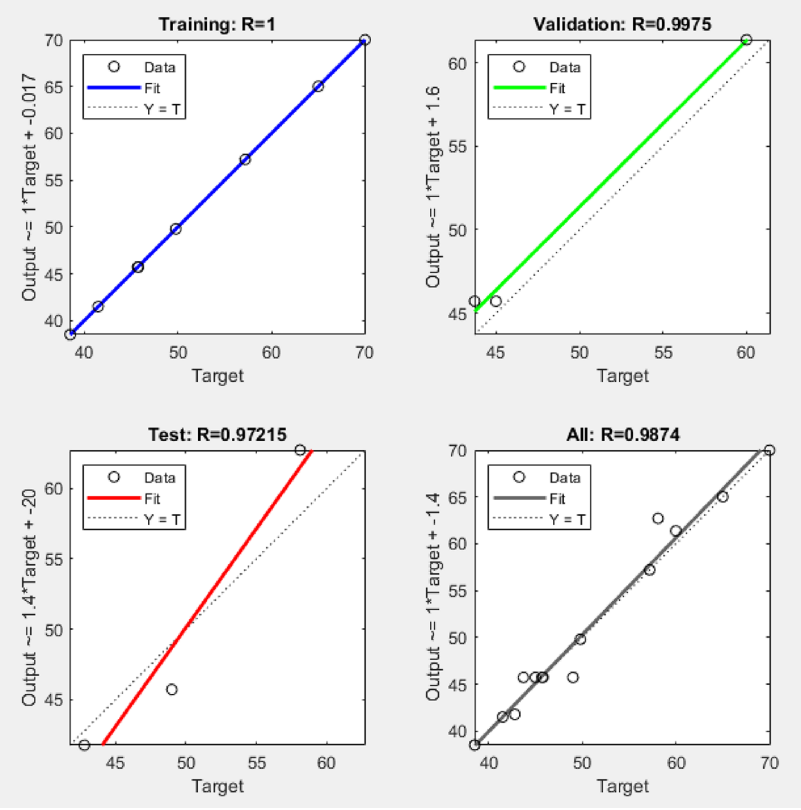

Figure 6. Regression plots for training, testing, validation, and overall data set for the developed ANN model.

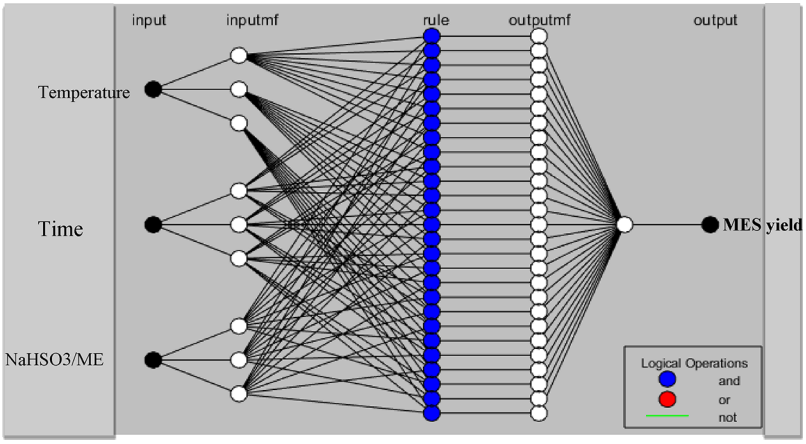

Figure 7. Developed ANFIS model framework.

unsaturated methyl ester contents, indicating that the intermediate product satisfied the minimum requirement of the ASTM and EN 14214 standard.[41]

3.2. Sulfonation Process Modeling via RSM. The CCD matrix and the estimated value of MES yield by the RSM model are shown in Table 7. The RSM model predicted a range of MES yields between 37.14 and 68.63%. The polynomial regression model obtained for the process using Design Expert version 7.0.0 is described by eq 19.

$$\text{MES yield } (\%) = +1233.11 - 10.39T - 220.40t - 363.29M + 0.81Tt + 1.44TM + 58.47tM + 0.03T^2 + 8.03t^2 - 12.43M^2 \quad (19)$$

where T is sulfonation temperature (°C), t is the sulfonation time (h), and M is the $NaHSO_3$/ME molar ratio (min).

Table 8 displays the ANOVA and statistical significance test outcomes for the model. The Fisher test (F value) and p value at a 95% degree of confidence were employed to determine statistical significance. The model's p value and F value are 0.0027 and 17.87, respectively, indicating that it is significant overall. All the model terms are significant except for the

https://doi.org/10.1021/acsomega.2c08117
ACS Omega 2023, 8, 19287−19301

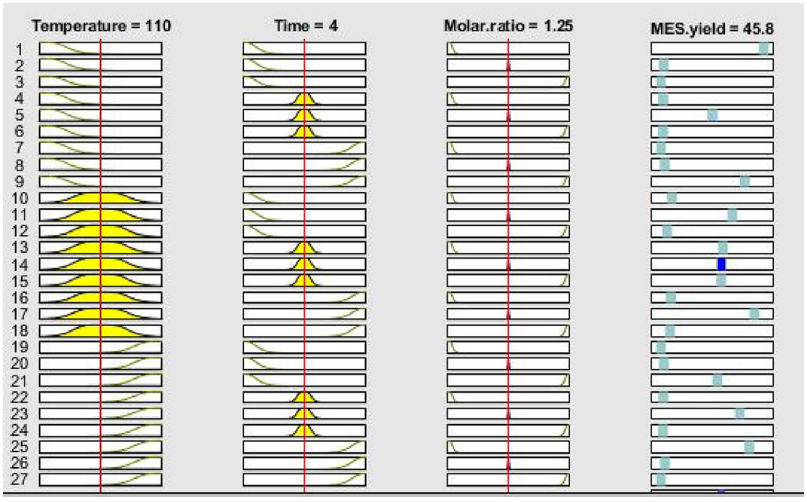

Figure 8. Developed ANFIS model rule viewer.

Figure 9. Experimental and predicted values vs run numbers for the ANFIS model.

$NaHSO_3$/ME molar ratio (M), interaction between sulfonation temperature and $NaHSO_3$/ME (TM), quadratic of sulfonation temperature (T^2), and quadratic of $NaHSO_3$/ME molar ratio (M^2). The model's high R^2 (0.9698) and adjusted R^2 (0.9685) values confirmed its validity. The Pareto chart was employed to estimate each model term's significance and their interactions (Figure 2). The significance of each model term on the chart depends on the length of the bar.[42] Hence, from the Pareto chart, the insignificant model term was the quadratic term of the sulfonation temperature followed by the interaction between sulfonation temperature and $NaHSO_3$/ME molar ratio term and the quadratic and linear terms of the $NaHSO_3$/ME molar ratio term, whereas other model terms are significant. This corroborates the ANOVA evaluations depicted in Table 8. The actual and predicted values have low variance, as indicated by the low coefficient of variance (CV), which is 5.66%. The signal/noise ratio is gauged by adequate precision; a value >4 is desirable.[43] The value of 13.606 computed in this work (Table 9) implies an adequate signal.

3.2.1. Variables' Interactive Effect on Sulfonation Process Response. Figure 3 depicts the interactive effect of temperature, time, and $NaHSO_3$/ME molar ratio on the sulfonation process. There was a corresponding increase in MES yield with increasing sulfonation temperature and time, as illustrated in Figure 3a. Temperature was thought to determine the extent of heat transfer by the catalyst (Al_2O_3) to improve the diffusion of

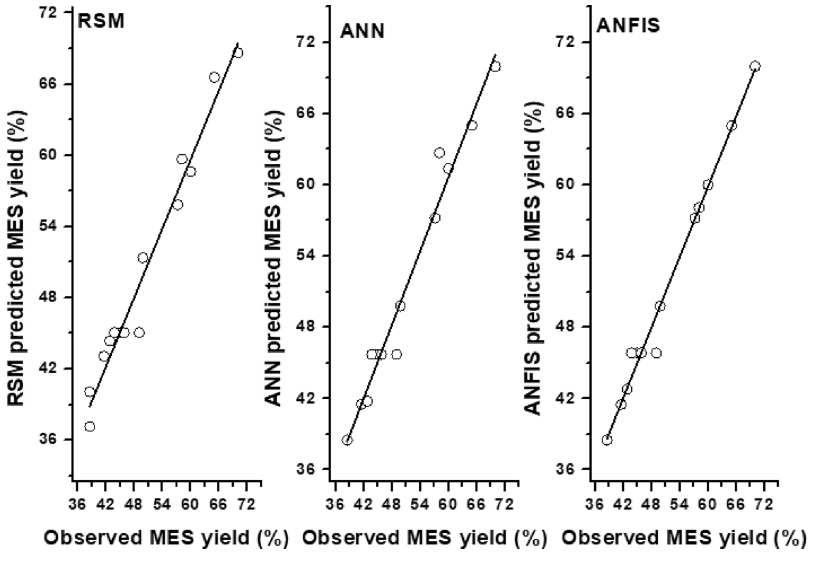

Figure 10. Experimental vs predicted values' parity plots for the developed models.

https://doi.org/10.1021/acsomega.2c08117
ACS Omega 2023, 8, 19287−19301

Table 10. Optimization Techniques and Model Validation

method	reaction temperature (°C)	reaction time (h)	$NaHSO_3$/ME (mol/mol)	predicted MES yield (%)	experimental MES yield (%)
RSM	101.38	3.06	1:1	65.43	67.03
RSM-PSO	96.84	2.68	1.18:1	67.25	68.01
ANN-PSO	99.16	2.68	0.99:1	72.35	73.22
ANFIS-PSO	96.84	2.68	0.92:1	74.82	77.96

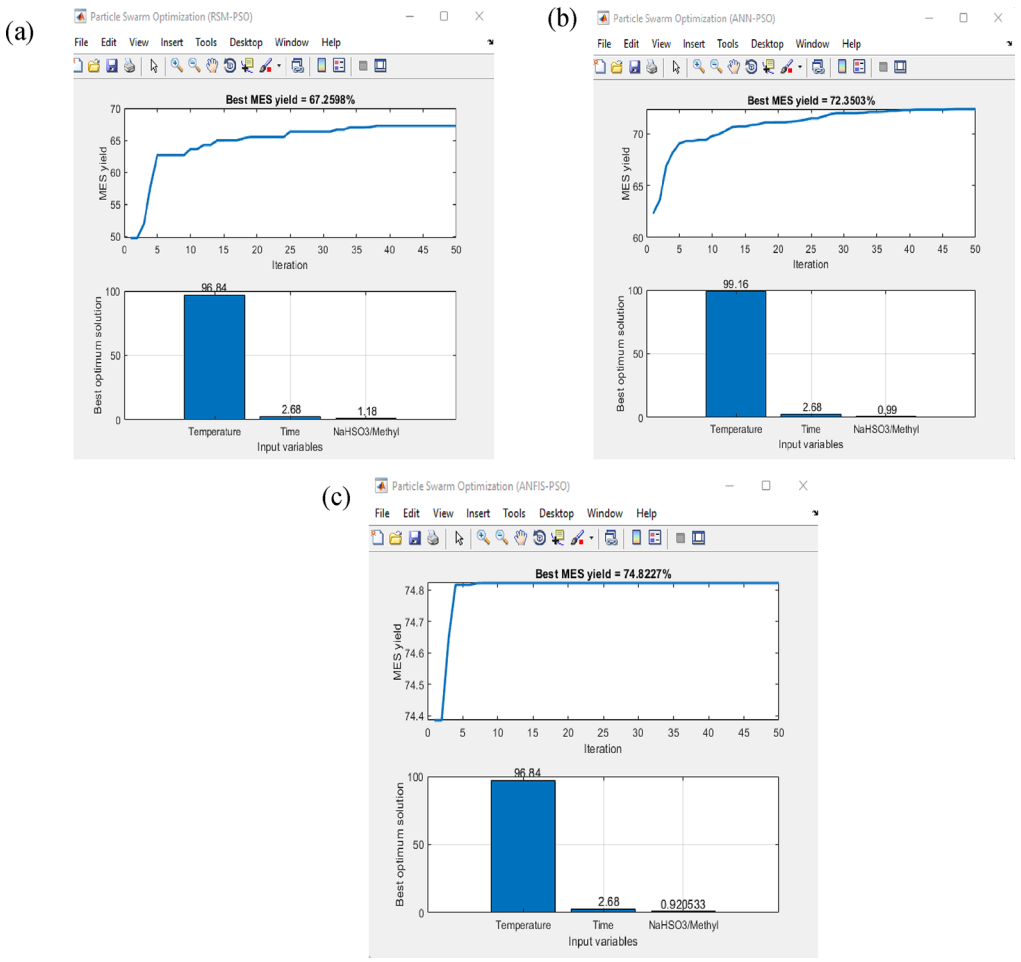

Figure 11. Convergence and optimization result plots for the PSO. (a) RSM model, (b) ANN model, and (c) ANFIS model.

the $NaHSO_3$ (sulfonating agent) into the liquid phase (methyl ester), thus increasing the reaction rate. This finding was consistent with previous research.[9]

The ME was sulfonated with $NaHSO_3$ at a fixed temperature of 110 °C to evaluate the combined effect of $NaHSO_3$/ME molar ratio and sulfonation time on MES yield. The MES yield decreased with increasing molar ratio of $NaHSO_3$ to ME and sulfonation time (Figure 3b). This result indicated that the highest MES yield was obtained at a low molar ratio of sulfonating agent to intermediate product, implying that there was no reaction of MES with unconsumed $NaHSO_3$ in the liquid phase.[9] However, the minimum MES yield obtained at a higher molar ratio of $NaHSO_3$ to ME suggested that a high concentration of unreacted sulfonating agent in the reaction medium drove the reaction toward the formation of more intermediates.[44] This observation was corroborated by Figure 3c (effect of $NaHSO_3$/ME molar ratio and temperature on MES yield), where the maximum MES yield was achieved at low $NaHSO_3$/ME molar ratio, confirming that sulfonation temperature was significant to MES yield (sulfonation process output variable).

3.3. Sulfonation Process Modeling via ANN. The experimental data set produced by the CCD was used to execute the neural network model. Fifteen experimental data points were adequately employed in total, of which 60% were engaged to train the network model, 20% to test it, and the remaining 35% to validate the model. Table 5 shows the predicted results by the developed ANN model. To compute the weights and biases for this network, the Levenberg–Marquardt (LM) back-propagation procedure was engaged during the training. The neural network was trained heuristically with different hidden neurons (2 to 20). The optimal hidden neuron selected was 10 because it gave the MSE and highest R as shown in Figure 4. In this study, the sulfonation process' network structure is shown in Figure 5, where 3 represents the input variables, 10 represents hidden neurons, and 1 represents the output (MES yield). The results of the regression for validation, training, testing, and overall are

https://doi.org/10.1021/acsomega.2c08117
ACS Omega 2023, 8, 19287−19301

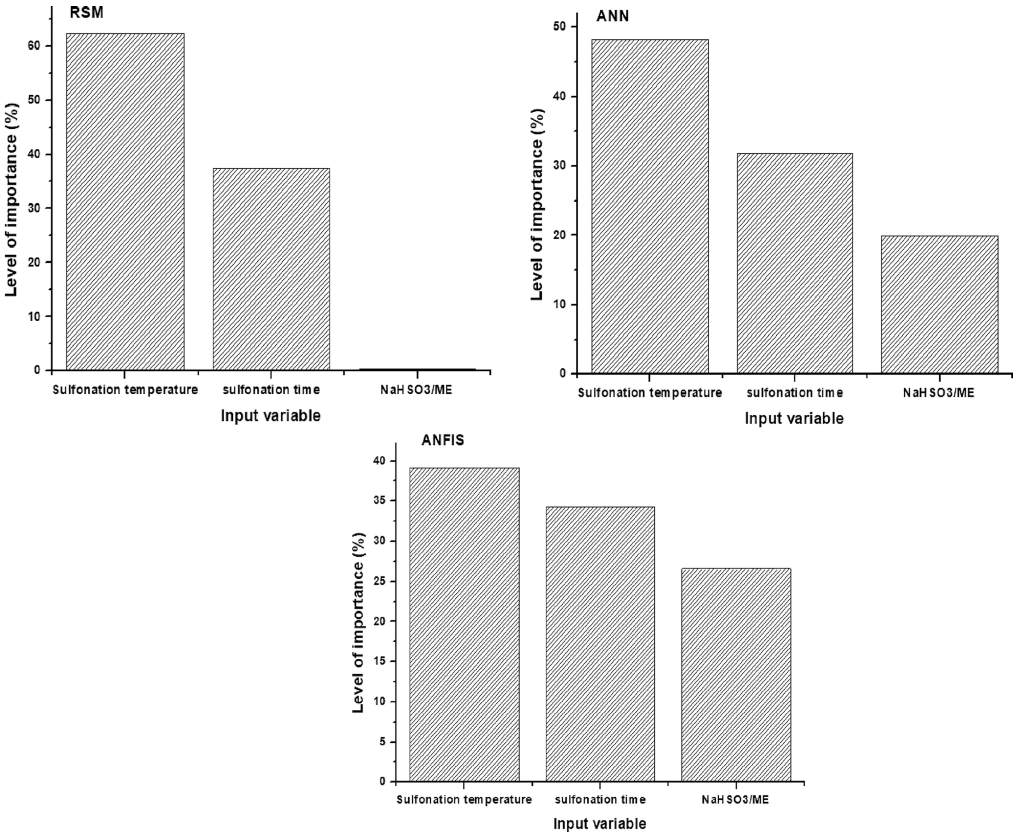

Figure 12. Level of importance of process input variables on MES yield.

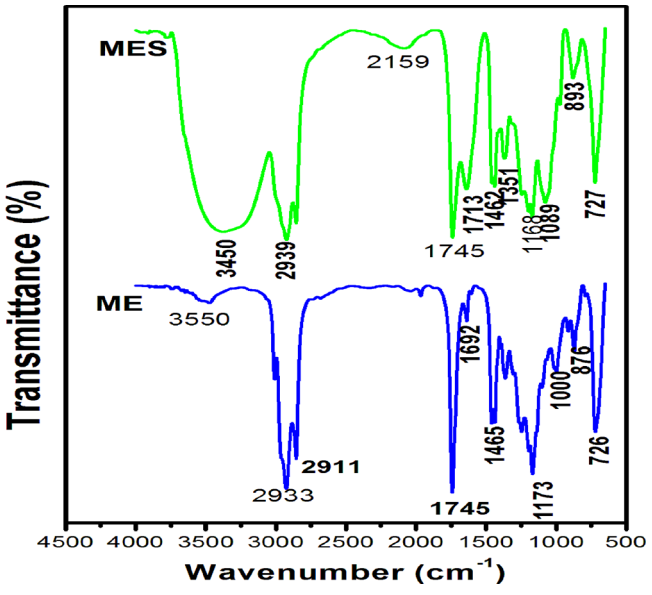

Figure 13. FTIR spectra of ME and MES samples.

displayed in Figure 6. The results revealed that the observed and predicted values had a good degree of agreement.

3.4. Sulfonation Process Modeling via ANFIS. Figure 7 presents the framework of the ANFIS model. About 27 (3 × 3 × 3) rules consisting of three linguistic terms, viz., low, medium, and high, were used for the ANFIS model (Figure 8). Table 9 displays the ANFIS model's predicted MES yields for various experimental conditions. Figure 9 depicts graphs of experimental and prognosticated values vs run numbers, illustrating the model's accuracy. The R, R^2, and adjusted R^2 values for the ANFIS model were 0.9943, 0.9886, and 0.9844, respectively, confirming a strong correlation between the experimental and predicted values. A good fit model is also defined by a high R^2 value.[45] This suggests that the developed model can account for 98.8% of the variation between experimental and prognosticated values.[46]

3.5. Developed Models' Performance Evaluation. By computing the MSE R, AAD, R^2, and adjusted R^2, it was statistically determined that the generated models were capable of predicting the MES yield. Table 9 displays the outcomes calculated from these statistical measures for the three models. Figure 10 illustrates the regression plots of predicted and observed values, which agree with the high values of R obtained for the three models (Table 9). According to some reports, the correlation between predicted and observed values should be at least 0.8.[45] Additionally, the three models' R^2 values were high, indicating strong model fitness.[45] The adjusted R^2 was utilized to verify R^2 overestimation, and all of the models' estimated values were high, demonstrating their importance. The error terms (MSE and AAD) computed for all the developed models have low values, demonstrating that all the models have good precision and accuracy. The ANFIS model was superior to RSM and ANN models, as indicated in Table 9, whereas the RSM model has the lowest precision and accuracy for predicting MES yield.

3.6. Optimization of the Input Process Variables for the Sulfonation Process. The process input variables (temperature of sulfonation, sulfonation time, and molar ratio of $NaHSO_3$/ME) were optimized using RSM, RSM-PSO, ANN-PSO, and ANFIS-PSO. Employing the developed models as objective functions, PSO was applied to obtain the

https://doi.org/10.1021/acsomega.2c08117
ACS Omega 2023, 8, 19287−19301

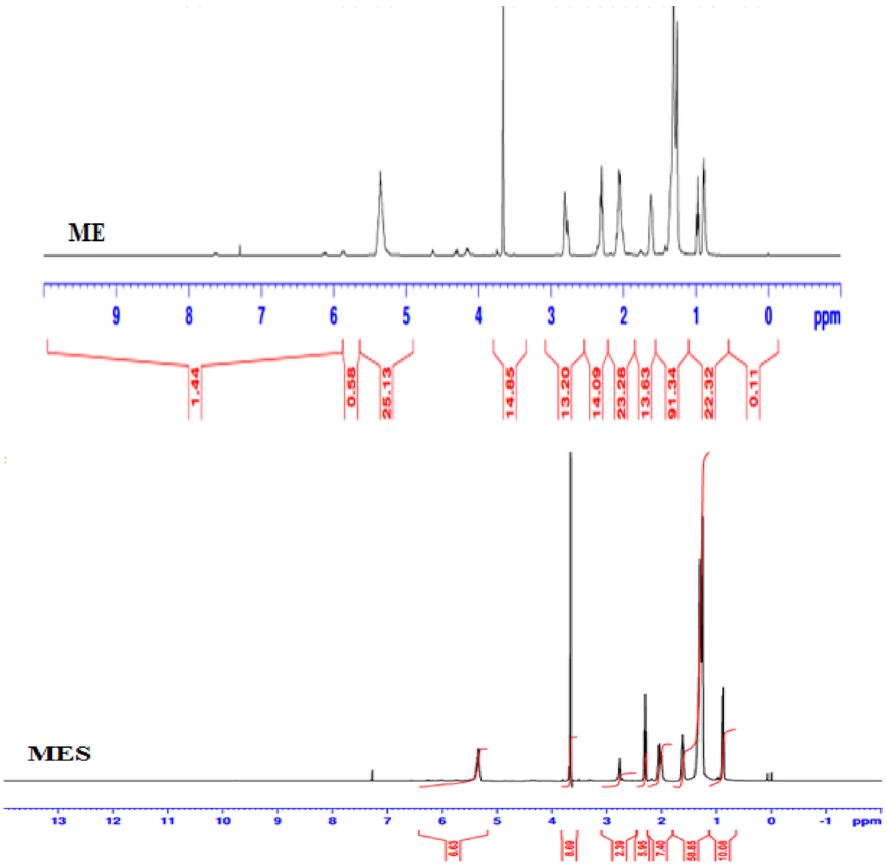

Figure 14. ^{1}H NMR spectra of ME and MES.

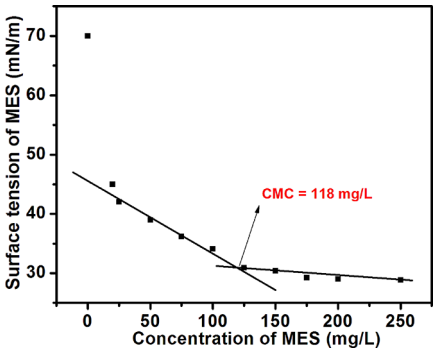

Figure 15. Surface tension−concentration plot for MES.

best combination of the investigated input process variable for the highest MES yield. The established optimum conditions for each of the techniques are presented in Table 10. Figure 11 displays the optimization result for RSM-PSO, ANN-PSO, and ANFIS-PSO. The estimated values were validated in duplicate in the laboratory, and the mean value of the MES yield is reported in Table 10. The order of the optimization is ranked as ANFIS-PSO, ANN-PSO, RSM-PSO, and RSM (see Table 10). ANFIS-PSO gave the highest MES yield (74.8%) under favorable conditions of reaction temperature 96.8 °C, reaction time 2.68 h, and molar ratio of $NaHSO_3$/ME molar ratio 0.92.

3.7. Sensitivity Analysis of the Input Variables on MES Yield. Figure 12 displays the sensitivity analysis for the ANFIS and ANN models. The outcomes exhibit a similar pattern to that of RSM, where sulfonation temperature is the most important input factor on the response (MES yield) followed by sulfonation time and finally $NaHSO_3$/ME molar ratio. It was observed that the levels of importance varied for the different modeling techniques (see Figure 12). Although the level of importance for $NaHSO_3$/ME molar ratio for the RSM model was very low compared to ANN and ANFIS, none of the process input factors, however, could be disregarded.

3.8. Analysis of MES Produced under Optimum Conditions. *3.8.1. FTIR Analysis.* Figure 13 presents the FTIR analysis conducted on both ME and MES to determine the functional groups. The FTIR spectra of ME and MES revealed some peaks around 2939−2911 cm^{-1}, indicating $-CH_3$ (methyl) stretching vibration.[4,13] Also, the peak at 1745 cm^{-1} (C═O stretching) appeared in the spectra of both samples, suggesting that the sulfonation process did not affect the ester group, as reported for ME and MES obtained from sesame oil.[1] The new peaks at 1351, 1168, and 1089 cm^{-1} on the spectrum of the UCO MES were all attributed to S═O vibration reductions, indicating that sulfonic acid ($-SO_3H$) was successfully incorporated into the MES structure in the form of C-SO_3H.[4] These FTIR data confirmed that the sulfonation product was methyl ester sulfonate.

3.8.2. ^{1}H NMR Analysis. The ^{1}H NMR results of the ME and MES samples are shown in Figure 14. The signals at around 0.88−0.97 ppm in the ME spectrum were attributed to the methyl (CH_3-) proton of the fatty acid chains, whereas the signals at around 1.41−2.10 ppm were attributed to the methylene ($-CH_2-$) protons of saturated acyl chains.[1] Peaks at 3.71 and 5.42 ppm, respectively, indicated the presence of protons of CH_3-O- in ester and −CH═CH of the vinyl group.[47] However, after the conversion of ME to MES via the sulfonation process, some signal disappeared while some new

https://doi.org/10.1021/acsomega.2c08117
ACS Omega 2023, 8, 19287−19301

Scheme 1. Mechanism for the Transesterification of UCO into Fatty Acid Methyl Esters[a]

$$TG + ROH \overset{catalyst}{\Longleftrightarrow} DG + RCOOR' \quad (1)$$

$$DG + ROH \overset{catalyst}{\Longleftrightarrow} MG + RCOOR' \quad (2)$$

$$MG + ROH \overset{catalyst}{\Longleftrightarrow} G + RCOOR' \quad (3)$$

(a)

$$TG + 3ROH \overset{catalyst}{\Longleftrightarrow} G + 3RCOOR' \quad (4)$$

(b)

$R' = carbon\ chain\ of\ fatty\ acid; R = alkyl\ group\ of\ alcohol; RCOOR' = methyl\ ester$

[a](a) Transesterification reaction steps. (b) Transesterification of triglyceride with methanol.

Scheme 2. Reaction Mechanism for the Sulfonation of Methyl Ester with $NaHSO_3$

$$RCH_2(CO_2)CH_3 + NaHSO_3 \rightarrow RCH(SO_3H)CO_2CH_3 \quad (1)$$

$$RCH(SO_3H)CO_2CH_3 + CH_3OH \rightarrow RCH(SO_3H)CO_2CH_3 + CH_3OH \quad (2)$$

$$RCH(SO_3H)CO_2CH_3 + NaOH \rightarrow RCH(SO_3Na)CO_2CH_3 + H_2O \quad (3)$$

signals were formed, indicating that the target product (MES) was successfully formed. New signals formed at 0.83 ppm (terminal methyl (CH_3-) proton), 2.38 ppm (allylic ($=CH-CH_2-CH=$) protons), 3.37 ppm ($-OCH_3-$ linked with the ester group), and 3.68 ppm (proton linked with carbon atom bearing the $-SO_3$ (sulfonate) group) were detected. Interestingly, the ^1H NMR signals of the produced MES confirmed the presence of methyl, ester, and sulfonate groups.

3.8.3. Surface Tension Analysis of MES. Figure 15 displays the plot of surface tension against MES concentration. The result revealed a decrease in surface tension with increasing MES concentration. However, the values of MES surface tension stabilized as saturation of solution/air interface with molecules of surfactant set in.[4] In addition to this, the values of the critical micelle concentration (CMC) and corresponding surface tension were estimated from Figure 15. The point where the descending and horizontal lines intercept was taken as the value of CMC. Regarding the results obtained, the values of the CMC and corresponding surface tension were 118 mg/L (0.118 g/L) and 32.1 mN/m, respectively. Comparing the MES synthesized in the current work and MES obtained from mango kernel oil by Sathi Reddy et al.,[48] the CMC of the former was slightly greater than the CMC of the latter (80 mg/L). However, the CMC of MES synthesized from castor oil using chlorosulfonic acid (sulfonating agent) was 205 mg/L,[49] and this was higher than the CMC of MES produced herein. The discrepancy might be due to the different source of intermediate product and sulfonating agent used. Nevertheless, MES with lower CMC often possesses improved hydrophobic surface and reduced surface tension capability as the surfactant molecules can arrange themselves closer to the surface.[4]

3.9. Reaction Mechanisms for Methanolysis of Used Cooking Oil and Sulfonation of Methyl Ester. Reaction Scheme 1 shows the mechanism for the transesterification of UCO into fatty acid methyl esters. During methanolysis of UCO in the presence of a catalyst (KOH), the triglycerides (TG) present in UCO convert to diglycerides (DG) followed by the conversion of DG to monoglycerides (MG) and then finally to glycerol (G). Overall, 1 mol TG reacts with 3 mol methanol in the presence of a KOH catalyst to produce 1 mol glycerol and 3 mol methyl esters (ME, desired product), which correspond to the various fatty acid methyl esters detected (see Table 6).

Scheme 2 displays the reaction mechanism for the sulfonation of fatty acid methyl esters with $NaHSO_3$. The hydrosulfite (SO_3H) anion replaces a hydrogen atom attached to the α-carbon of methyl ester, and Na^+ is removed during sulfonation, resulting in the formation of an intermediate product (MESA), which is purified by methanol and subsequently neutralized by NaOH solution at controlled conditions (pH and temperature) to produce methyl ester sulfonate ($RCH(SO_3Na)CO_2CH_3$) and water.

4. CONCLUSIONS

This work focused on the significance of selecting the right modeling and optimization strategies to convert UCO to MES through the transesterification−sulfonation process. Detailed modeling of the process was executed using ANFIS, ANN, and RSM. Moreover, RSM, RSM-PSO ANN-PSO, and ANFIS-PSO were used in optimizing the three investigated input process variables (reaction temperature, sulfonation time, and $NaHSO_3$/methyl ester molar ratio) to obtain the highest MES yield. According to statistical measures for evaluating the efficiency of the created models, the RSM model recorded the least efficiency in predicting MES yield (R = 0.9846, MSE = 2.7094, and AAD = 2.9508%). The ANFIS model outperformed the ANN model (R = 0.9874, MSE = 2.6282, and AAD = 1.7184%) in terms of R, MSE, and AAD. The results of the optimization demonstrate that ANFIS-PSO provided the best combination of operation parameters (sulfonation temperature 96.84 °C, sulfonation time 2.68 h, and $NaHSO_3$/ME molar ratio 0.92:1 (mol/mol)) with the highest MES yield (74.82%). Finally, sensitivity analysis of the input variables on MES yield depicts that the ranking of the level of importance of the process variables is sulfonation temperature > sulfonation time > $NaHSO_3$/ME molar ratio.

AUTHOR INFORMATION

Corresponding Authors

Adeyinka Sikiru Yusuff − *Department of Chemical and Petroleum Engineering, College of Engineering, Afe Babalola University, Ado-Ekiti 23438, Nigeria*; orcid.org/0000-0002-6630-6411; Email: yusuffas@abuad.edu.ng

Niyi Babatunde Ishola − *Department of Chemical Engineering, Faculty of Technology, Obafemi Awolowo University, Ile-Ife 23438, Nigeria*; Email: isholaniyi10@gmail.com

Author

Afeez Olayinka Gbadamosi − *Department of Petroleum Engineering, College of Petroleum and Geosciences, King Fahd University of Petroleum and Minerals, 31261 Dhahran, Saudi Arabia*

Complete contact information is available at: https://pubs.acs.org/10.1021/acsomega.2c08117

https://doi.org/10.1021/acsomega.2c08117
ACS Omega 2023, 8, 19287−19301

Notes

The authors declare no competing financial interest.

■ ACKNOWLEDGMENTS

The first author thanks Afe Babalola University Ado-Ekiti, Nigeria, for providing facilities and financial support for this research.

■ REFERENCES

(1) Soy, R. C.; Kipkemboi, P. K.; Kiplangat, R. Synthesis, characterization and evaluation of solution properties of Sesame fatty acid methyl ester sulfonate. *ACS Omega* **2020**, *5*, 28643−28655.
(2) Maurad, Z. A.; Idris, Z.; Ghazali, R. Performance of palm-based $C_{16/18}$ methyl ester sulphonate (MES) in liquid detergent formulation. *J. Oleo Sci.* **2017**, *66*, 677−687.
(3) Tan, Y. H.; Abdullah, M. O.; Nolasco-Hipolito, C.; Taufiq-Yap, Y. H. Waste ostrich- and chicken-eggshells as heterogeneous base catalyst for biodiesel production from used cooking oil: Catalyst characterization and biodiesel yield performance. *Appl. Energy* **2015**, *160*, 58−70.
(4) Jin, Y.; Tian, S.; Guo, J.; Ren, X.; Li, X.; Gao, S. Synthesis, characterization and exploratory application of anionic surfactant fatty acid methyl ester sulfonate from waste cooking oil. *J. Surfactants Deterg.* **2016**, *19*, 467−475.
(5) Moyo, L. B.; Iyuke, S. E.; Muvhiwa, R. F.; Simate, G. S.; Hlabangana, N. Application of response surface methodology for optimization of biodiesel production parameters from waste cooking oil using a membrane reactor. *S. Afr. J. Chem. Eng.* **2021**, *35*, 1−7.
(6) Yusuff, A. S.; Adeniyi, O. D.; Olutoye, M. A.; Akpan, U. G. Performance and Emission Characteristics of Diesel Engine Fuelled with Waste Frying Oil Derived Biodiesel-Petroleum Diesel Blend. *Int. J. Eng. Res. Afr.* **2017**, *32*, 100−111.
(7) Yusuff, A. S.; Porwal, J.; Bhonsle, A. K.; Rawat, N.; Atray, N. Valorization of used cooking oil as a source of anionic surfactant fatty acid methyl ester sulfonate: process optimization and characterization studies. *Biomass Convers. Biorefin.* **2021**, DOI: 10.1007/s13399-021-01663-y.
(8) Kumar, S.; Saxena, N.; Mandal, A. Synthesis and evaluation of physicochemical properties of anionic polymeric surfactant derived from Jatropha oil for application in enhanced oil recovery. *J. Ind. Eng. Chem.* **2016**, *43*, 106−116.
(9) Xie, T.; Zheng, C.; Wang, C.; Zhang, L. Preparation of methyl ester sulfonates based on sulfonation in a falling film microreactor from hydrogenated palm oil methyl esters with gaseous SO_3. *Ind. Eng. Chem. Res.* **2013**, *52*, 3714−3722.
(10) Permdani, R. L.; Ibadurrohman, M.; Slamet, M. Utilization of waste cooking oil as raw material for synthesis of methyl ester sulfonates (MES) surfactant. *IOP Conf. Ser.: Earth Environ. Sci.* **2018**, *105*, No. 012036.
(11) Jiang, H.; Wang, W. Source analysis of dio-sodium salt in fatty acid methyl ester sulfonate and amelioration. *Chem. Eng. Prog.* **2014**, *31*, 1134−1136.
(12) Wibowo, A. D. K.; Yoshi, L. A.; Handayani, A. S.; Joelianingsil. Synthesis of polymeric surfactant from palm oil methyl ester for enhanced oil recovery application. *Colloid Polym. Sci.* **2021**, *299*, 81−92.
(13) Zhou, J.; Sun, Y.; Zhu, K.; Serio, M. D.; Zhang, Y.; Sun, J.; Wu, H.; Ding, L.; Liang, H.; Zhang, Y.; Sun, J.; Wu, H.; Ding, L.; Liang, H. Influence of sulfonic acid group on the performance of castor oil based methyl ester exthoxylate sulfonate. *J. Dispersion Sci. Technol.* **2018**, *39*, 1−6.
(14) Mansour, M.; Ghaffari, M.; Mostafa, K. Comparison of response surface methodology and artificial neural network in predicting the microwave-assisted extraction procedure to determine zinc in fish muscles. *Food. Nutri. Sci.* **2011**, *31*, 34−39.
(15) Huang, K. C.; Li, Y.; Kuo, C. H.; Twu, Y. K.; Shieh, C. J. Highly efficient synthesis of an emerging lipophilic antioxidant: 2-ethylhexyl ferulate. *Molecules* **2016**, *21*, 478.
(16) Kuo, C.-H.; Liu, T.-A.; Chen, J.-C.; Chang, C.-M. J.; Shieh, C.-J. Response surface methodology and artificial neural network optimized synthesis of enzymatic 2-phenylethyl acetate in a solvent-free system. *Biocatal. Agric. Biotechnol* **2014**, *3*, 1−6.
(17) Betiku, E.; Ishola, N. B. Optimization of sorrel oil biodiesel production by base heterogeneous catalyst from kola nut pod husk: Neural intelligence-genetic algorithm versus neuro-fuzzy-genetic algorithm. *Environ. Prog. Sustainable Energy* **2020**, *39*, No. e13393.
(18) Betiku, E.; Odude, V. O.; Ishola, N. B.; Bamimore, A.; Osunleke, A. S.; Okeleye, A. A. Predictive capability evaluation of RSM, ANFIS and ANN: a case of reduction of high free fatty acid of palm kernel oil via esterification process. *Energy Convers. Manage.* **2016**, *124*, 219−230.
(19) Betiku, E.; Osunleke, A. S.; Odude, V. O.; Bamimore, A.; Oladipo, B.; Okeleye, A. A.; Ishola, N. B. Performance evaluation of adaptive neuro-fuzzy inference system, artificial neural network and response surface methodology in modeling biodiesel synthesis from palm kernel oil by transesterification. *Biofuels* **2021**, *12*, 339−354.
(20) Rajendra, M.; Jena, P. C.; Raheman, H. Prediction of optimized pretreatment process parameters for biodiesel production using ANN and GA. *Fuel* **2009**, *88*, 868−875.
(21) Ishola, N. B.; McKenna, T. F. L. Influence of process parameters on the gas phase polymerization of ethylene: RSM or ANN Statistical Methods? *Macromol. Theory Simul.* **2021**, *30*, 2100059.
(22) Maleki, A.; Safdari Shadloo, M.; Rahmat, A. Application of artificial neural networks for producing an estimation of high-density polyethylene. *Polymer* **2020**, *12*, 2319.
(23) Yusuff, A. S.; Ishola, N. B.; Gbadamosi, A. O.; Thompson-Yusuff, K. A. Pumice-supported ZnO-photocatalyzed degradation of organic pollutant in textile effluent: optimization by response surface methodology, artificial neural network, and adaptive neural-fuzzy inference system. *Environ. Sci. Pollut. Res.* **2022**, *29*, 25138−25156.
(24) Malik, Z.; Rashid, K. Comparison of optimization by response surface methodology with neurofuzzy methods. *IEEE Trans. Magn.* **2000**, *36*, 241−257.
(25) Chizoo, E.; Augustine, S. C.; Chukwu, E. G.; Gerald, U. Adaptive neuro-fuzzy inference system-genetic algorithm versus response surface methodology-desirability function algorithm modelling and optimization of biodiesel synthesis from waste chicken fat. *J. Taiwan Inst. Chem. Eng.* **2022**, *136*, 104389.
(26) Ighose, B. O.; Adeleke, I. A.; Damos, M.; Junaid, H. A.; Okpalaeke, K. E.; Betiku, E. Optimization of biodiesel production from Thevetia peruviana seed oil by adaptive neuro-fuzzy inference system coupled with genetic algorithm and response surface methodology. *Energy Convers. Manage.* **2017**, *132*, 231−240.
(27) Ishola, N. B.; Adeyemi, O. O.; Adesina, A. J.; Odude, V. O.; Oyetunde, O. O.; Okeleye, A. A.; Soji-Adekunle, A. R.; Betiku, E. Adaptive neuro-fuzzy inference system-genetic algorithm vs. response surface methodology: A case of optimization of ferric sulfate-catalyzed esterification of palm kernel oil. *Process Saf. Environ. Prot.* **2017**, *111*, 211−220.
(28) Mostafaei, M.; Javadikia, H.; Naderloo, L. Modeling the effects of ultrasound power and reactor dimension on the biodiesel production yield: Comparison of prediction abilities between response surface methodology (RSM) and adaptive neuro-fuzzy inference system (ANFIS). *Energy* **2016**, *115*, 626−636.
(29) Hariram, V.; Bose, A.; Seralathan, S. Dataset on optimized biodiesel production from seeds of Vitis vinifera using ANN, RSM and ANFIS. *Data Brief* **2019**, *25*, 104298.
(30) Ishola, N. B.; Okeleye, A. A.; Osunleke, A. S.; Betiku, E. Process modeling and optimization of sorrel biodiesel synthesis using barium hydroxide as a base heterogeneous catalyst: appraisal of response surface methodology, neural network and neuro-fuzzy system. *Neural. Comput. Appl.* **2019**, *31*, 4929−4943.
(31) Rodriguez, M.; Montgomery, D. C.; Borror, C. M. Generating experimental designs involving control and noise variables using genetic algorithms. *Qual. Reliab. Eng. Int.* **2009**, *25*, 1045−1065.

https://doi.org/10.1021/acsomega.2c08117
ACS Omega 2023, 8, 19287−19301

(32) Shanmugaprakash, M.; Sivakumar, V. Development of experimental design approach and ANN-based models for determination of Cr (VI) ions uptake rate from aqueous solution onto the solid biodiesel waste residue. *Bioresour. Technol.* **2013**, *148*, 550−559.
(33) Sarve, A.; Sonawane, S. S.; Varma, M. N. Ultrasound assisted biodiesel production from sesame (Sesamum indicum L.) oil using barium hydroxide as a heterogeneous catalyst: Comparative assessment of prediction abilities between response surface methodology (RSM) and artificial neural network (ANN). *Ultrason. Sonochem.* **2015**, *26*, 218−228.
(34) Jacob, S.; Banerjee, R. Modeling and optimization of anaerobic codigestion of potato waste and aquatic weed by response surface methodology and artificial neural network coupled genetic algorithm. *Bioresour. Technol.* **2016**, *214*, 386−395.
(35) Jang, J.-S. R. ANFIS: adaptive-network-based fuzzy inference system. *IEEE Trans. Syst. Man Cybern. Syst.* **1993**, *23*, 665−685.
(36) Farjam, A.; Omid, M.; Akram, A.; Fazel Niari, Z. A neural network based modeling and sensitivity analysis of energy inputs for predicting seed and grain corn yields. *J. Agric. Sci. Technol.* **2014**, *16*, 767−778.
(37) Dhawane, S. H.; Bora, A. P.; Kumar, T.; Halder, G. Parametric optimization of biodiesel synthesis from rubber seed oil using iron doped carbon catalyst by Taguchi approach. *Renew. Energy* **2017**, *105*, 616−624.
(38) Garson, D. G. Interpreting neural network connection weights. *AI expert* **1991**, *6*, 46−51.
(39) Bassam, A.; May Tzuc, O.; Escalante Soberanis, M.; Ricalde, L.; Cruz, B. Temperature estimation for photovoltaic array using an adaptive neuro fuzzy inference system. *Sustainability* **2017**, *9*, 1399.
(40) Avramović, J. M.; Veličković, A. V.; Stamenković, O. S.; Rajković, K. M.; Milić, P. S.; Veljković, V. B. Optimization of sunflower oil ethanolysis catalyzed by calcium oxide: RSM versus ANN-GA. *Energy Convers. Manage.* **2015**, *105*, 1149−1156.
(41) Ho, W. W. S.; Ng, H. K.; Gan, S.; Tan, S. H. Evaluation of palm oil mill fly ash supported calcium oxide as a heterogeneous base catalyst in biodiesel synthesis from crude palm oil. *Energy Convers. Manage.* **2014**, *88*, 1167−1178.
(42) Betiku, E.; Akintunde, A. M.; Ojumu, T. V. Banana peels as a biobase catalyst for fatty acid methyl esters production using Napoleon's plume (Bauhinia monandra) seed oil: A process parameters optimization study. *Energy* **2016**, *103*, 797−806.
(43) Betiku, E.; Okunsolawo, S. S.; Ajala, S. O.; Odedele, O. S. Performance evaluation of artificial neural network coupled with generic algorithm and response surface methodology in modeling and optimization of biodiesel production process parameters from shea tree (Vitellaria paradoxa) nut butter. *Renew. Energy* **2015**, *76*, 408−417.
(44) Sahila, S.; Qadariyah, L.; Mahfud, M. The study on factors affecting the synthesis of methyl ester sulfonate from palm oil using CaO catalyst with microwave-assisted. *J. Phys.: Conf. Ser.* **2021**, *1845*, No. 012004.
(45) Joglekar, A.M.; May, A.; Graf, E.; Saguy, I. Product excellence through experimental design. *Food product and development: From concept to the marketplace*; Springer Science & Business Media: 1987, 211−230.
(46) Betiku, E.; Adepoju, T. F. Methanolysis optimization of sesame (*Sesamum indicum*) oil to biodiesel and fuel quality characterization. *Int. J. Energy Environ. Eng.* **2013**, *4*, 1−8.
(47) Tariq, M.; Ali, S.; Ahmad, F.; Ahmad, F.; Zafar, M.; Khalid, N.; Khan, M. A. Identification, FTIR, NMR (^{1}H and ^{13}C) and GC/MS studies of fatty acid methyl esters in biodiesel from rocket seed oil. *Fuel Process. Technol.* **2011**, *92*, 336−341.
(48) Sathi Reddy, K.; Yahya, K. M.; Archana, K.; Gopal Reddy, M.; Hameeda, B. Utilization of mango kernel oil for the rhamnolipid production of pseudomonas aeruginosa DRI towards its application as bio control agent. *Bioresour. Technol.* **2016**, *221*, 291−299.
(49) Babu, K.; Maurya, N. K.; Mandal, A.; Saxena, V. K.; Indian School of Mines, India; Indian School of Mines, India. Synthesis and characterization of sodium methyl ester sulfonate for chemically-enhanced oil recovery. *Braz. J. Chem. Eng.* **2015**, *32*, 795−803.

https://doi.org/10.1021/acsomega.2c08117
ACS Omega 2023, 8, 19287−19301